Journal of Sound and Vibration (1999) 224(3), 489–503
Article No. jsvi.1999.2192, available online at http://www.idealibrary.com on IDEAL®

EFFECTS OF STRUCTURAL DEFORMATIONS OF THE CRANK-SLIDER MECHANISM ON THE ESTIMATION OF THE INSTANTANEOUS ENGINE FRICTION TORQUE

N. G. CHALHOUB, H. NEHME AND N. A. HENEIN

Department of Mechanical Engineering, Wayne State University, Detroit, MI 48202, *U.S.A.*

AND

W. BRYZIK

U.S. Army Tank-Automotive RDE Center, AMSTA-R, Warren, MI 48397-5000, *U.S.A.*

(*Received* 15 *July* 1998 *and in final form* 14 *January* 1999)

The focus on the current study is to assess the effects of structural deformations of the crankshaft/connecting-rod/piston mechanism on the computation of the instantaneous engine friction torque. This study is performed in a fully controlled environment in order to isolate the effects of structural deformations from those of measurement errors or noise interference. Therefore, a detailed model, accounting for the rigid and flexible motions of the crank-slider mechanism and including engine component friction formulations, is considered in this study. The model is used as a test bed to generate the engine friction torque, T_{fa}, and to predict the rigid and flexible motions of the system in response to the cylinder gas pressure. The torsional vibrations and the rigid body angular velocity of the crankshaft, as predicted by the detailed model of the crank-slider mechanism, are used along with the engine load torque and the cylinder gas pressure in the (P–ω) method to estimate the engine friction torque, T_{fe}. This method is well suited for the purpose of this study because its formulation is based on the rigid body model of the crank-slider mechanism. The digital simulation results demonstrate that the exclusion of the structural deformations of the crank-slider mechanism from the formulation of the ($P-\omega$) method leads to an overestimation of the engine friction torque near the top-dead-center (TDC) position of the piston under firing conditions. Moreover, for the remainder of the engine cycle, the estimated friction torque exhibits large oscillations and takes on positive numerical values as if it is inducing energy into the system. Thus, the adverse effects of structural deformations of the crank-slider mechanism on the estimation of the engine friction torque greatly differ in their nature from one phase of the engine cycle to another.

1. INTRODUCTION

Reductions in engine frictional losses improve the engine efficiency, which enhances the vehicle fuel consumption and reduces the tail pipe HC, CO, and NO_x

0022-460X/99/280489 + 15 $30.00/0

emissions [1, 2]. This goal cannot be achieved without the development of reliable methods for measuring instantaneous frictional losses in engines [3–6]. Moreover, the availability of such tools would enable designers to develop a better understanding of the lubrication regimes under which engine components may operate. This knowledge base will aid engineers in modifying their designs to increase the life expectancy of engine components.

A common method for measuring engine frictional losses is the "motoring test". The engine is motored by a dynamometer and the generated torque that maintains a constant engine speed is considered to be the friction torque. The major drawback of this approach stems from the fact that the measured torque accounts for the combined effects of heat losses, pumping work, accessory loads and frictional losses [5]. Furthermore, the motoring test does not represent actual engine firing conditions which result in higher back pressures on the compression rings, large side thrusts on piston skirts, significant impacts and heavier loads on main engine bearings. Moreover, the high temperatures associated with engine firing conditions can significantly change the viscosity of the lubricating oil films. In addition, the thermal expansions of the engine components can induce variations in the clearances between the rubbing surfaces. Therefore, the characteristics of the lubricating regimes under engine firing conditions greatly differ from those under motoring conditions [6, 7].

Other approaches for determining the average value of the overall frictional losses in internal combustion engines are the Willan line method, the Morse method and the indicated work method. Although these techniques consider engine firing conditions; however, they are limited in their scope of applications to steady state operating conditions [6].

The (P–ω) method determines the instantaneous friction torque of internal combustion engines under both transient and steady state modes of operations [8]. It is a model-based approach in which the total frictional losses of the engine are computed from a rigid body model of the crankshaft/connecting-rod/piston mechanism. This methodology relies on accurate measurements of the cylinder gas pressure, P, and the crankshaft angular velocity, ω.

Similarly, the instantaneous mean effective pressure (IMEP) method determines the piston-assembly frictional losses based on a rigid body model of the piston and a portion of the connecting-rod [5]. Again, this methodology requires accurate measurements of the cylinder gas pressure, the connecting-rod forces and the crankshaft angular velocity.

Note that both the (P–ω) and the IMEP techniques do not require structural modifications of the engine [9, 10]. They can also be implemented under either motoring or firing conditions. However, at specific periods during the engine cycle, both methods have led to erroneous results by yielding positive numerical values for the friction force/torque. The accuracy of these techniques heavily depends on the crank-slider model used in the computation of the frictional losses. Neglecting the piston slap, piston tilting and structural deformations from the dynamic equations of the crank-slider mechanism renders both approaches to be inaccurate, particularly, at high engine speeds. The spikes observed in experimental friction data have been attributed in the literature to impacts that are induced by the piston

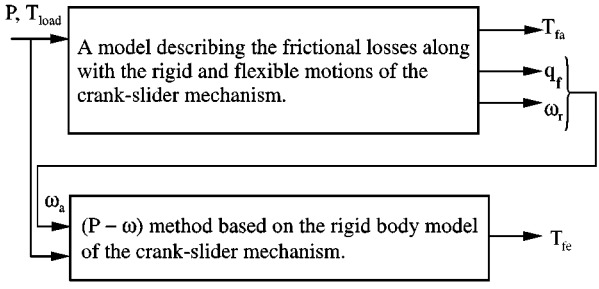

Figure 1. Strategy for assessing the effects of structural deformations.

slap. In addition, the friction curve is shown to become hardly recognizable at high engine speeds due to the effect of the crank-slider structural deformations.

In an attempt to consider the effect of structural deformations, Taraza and his co-workers [11] have mounted two optical encoders on the crankshaft and used a lumped mass model of the crank-slider mechanism to approximate the rigid body angular velocity of the crankshaft. The latter is then used in the (P–ω) method to determine the engine friction torque. This procedure, which served to improve the accuracy of the (P–ω) technique, can only be implemented under steady state operating conditions of the engine and cannot take into consideration more than one elastic mode of the crankshaft.

The purpose of this study is to assess the effects of structural deformations of the crank-slider mechanism on the computation of the instantaneous engine friction torque. This study has been performed in a fully controlled environment in order to isolate the effects of structural deformations from those of measurement errors or noise interference. A detailed model, accounting for the rigid and flexible motions of the crank-slider mechanism and including Rezeka and Henein's [12] engine component friction formulations, is considered in this study. The model is used as a test bed to generate the instantaneous friction torque of the engine, T_{fa}, the rigid body angular velocity of the crankshaft, ω_r, and the structural deformations of the crankshaft/connecting-rod/piston mechanism, $\mathbf{q}_f$ (see Figure 1).

The (P–ω) method is originally formulated to have the rigid body angular velocity of the crankshaft, ω_r, the cylinder gas pressure, P, and the engine load torque, T_{load}, as inputs. Instead, the measured signals of ω_a, P and T_{load} are used. ω_a is usually determined from the signal of an optical encoder that is mounted on the crankshaft. Barring any measurement errors, the difference between ω_a and ω_r stems from the crankshaft torsional vibrations present in the optical encoder signal. Therefore, the objective of this study is to examine the effects of the crankshaft structural deformations on the estimated friction torque of the engine, T_{fe}, under the controlled environment that is depicted in Figure 1.

The detailed model of the crankshaft/connecting-rod/piston mechanism along with the formulations for determining the frictional losses of the engine components is included in section 2. Subsequently, the (P–ω) method is described and the digital simulation results are presented. In section 4, the work is summarized and the main conclusions are highlighted.

2. DYNAMIC MODEL OF THE CRANK-SLIDER MECHANISM

The distributed mass model, presented in this section, describes the combined rigid and flexible motions of the crankshaft/connecting-rod/piston mechanism for a single cylinder internal combustion engine (see Figure 2). The formulation ignores the piston slap and the piston tilting. It treats the piston as a rigid body that can only move along the centerline of the cylinder.

The model takes into consideration the first three elastic modes for each of the torsional vibration, ϕ, and the out-of-plane transverse deformation, W_{cs}, of the crankshaft. It treats the counterweights, the flywheel and the crank gear as rigid

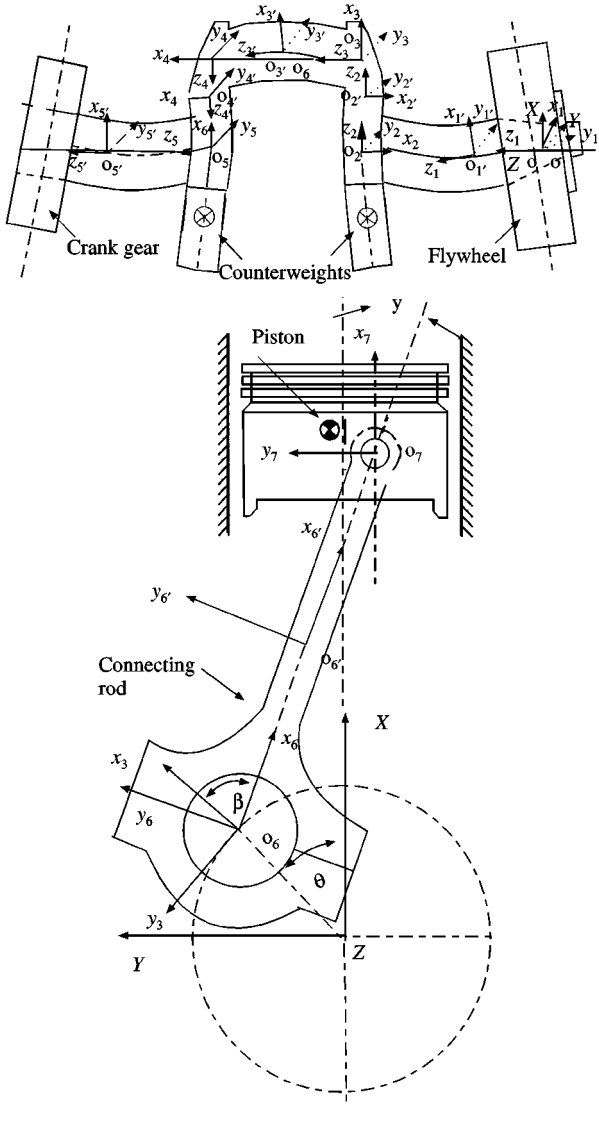

Figure 2. A schematic diagram of the crank-slider mechanism.

bodies. Since the connecting rod is stiffer than the crankshaft then only the first elastic mode of its out-of-plane transverse deformation, W_{cr}, is included in the derivations. The structural flexibility terms are discretized by using the assumed modes method [13]. The admissible functions in the ϕ and W_{cs} approximations are selected to be the eigenfunctions of the crankshaft, including the counterweights, the flywheel and the crank gear [14]. Note that the transverse deformation and the torsional vibration of the crankshaft are highly coupled. For any two adjacent beam elements of the crankshaft (see Figure 2), what may constitute the torsional vibration of one element becomes the slope of the transverse deformation of the other.

Similarly, the admissible function in the approximation of W_{cr} is considered to be the eigenfunction of a pinned–pinned beam which is readily available in the literature.

Besides the inertial frame, (X, Y, Z), seven non-inertial rotating co-ordinate systems, $\{(x_i, y_i, z_i), i = 1, \ldots, 7\}$, are assigned to the piston, the connecting rod and the five beam elements of the crankshaft (see Figure 2). Additional six floating co-ordinate systems, $\{(x_{i'}\ y_{i'},\ z_{i'}),\ i' = 1, \ldots, 6\}$, are assigned to the compliant five-beam elements of the crankshaft and the connecting-rod. The extended absolute position vector of any point on the ith beam element of the crankshaft can be systematically determined from

$$\{\mathbf{r}_{cs}^{(i)\mathrm{T}} \mid 1\} = \left[\prod_{j=1}^{i} T_{j-1}^{j}\right] T_{i}^{i'} \{x_{i'}\ y_{i'}\ 0 \mid 1\}^{\mathrm{T}}, \tag{1}$$

where T_{j-1}^{j} defines the origin and orientation of the jth co-ordinate system with respect to the $(j-1)$th frame in the nominal rigid body configuration of the crankshaft. $T_{i}^{i'}$ represents the location of $O_{i'}$ and the orientation of $(x_{i'}, y_{i'}, z_{i'})$ with respect to (x_i, y_i, z_i). Similarly, the position vectors of any point on the connecting rod and of the mass center of the piston can be expressed as

$$\{\mathbf{r}_{cr}^{\mathrm{T}} \mid 1\}^{\mathrm{T}} = T_{0}^{3}\ T_{\bar{3}}^{\bar{3}'}\ T_{\bar{3}}^{6}\ T_{6}^{6'}\ \{0\ y_{6'}\ z_{6'} \mid 1\}^{\mathrm{T}}, \tag{2}$$

$$\{\mathbf{r}_{p}^{\mathrm{T}} \mid 1\}^{\mathrm{T}} = T_{0}^{3}\ T_{\bar{3}}^{\bar{3}'}\ T_{\bar{3}}^{6}\ T_{6}^{6'_e}\ T_{6'_e}^{7}, \{x_7^*\ y_7^*\ z_7^* \mid 1\}^{\mathrm{T}}, \tag{3}$$

where $(x_{\bar{3}'}, y_{\bar{3}'}, z_{\bar{3}'})$ and $(x_{6'_e}, y_{6'_e}, z_{6'_e})$ represent floating co-ordinate systems whose origins are fixed at $z_3 = L_3/2$ and $x_6 = L_6$, respectively.

Next, the kinetic and potential energy expressions are determined from

$$K.E. = \frac{1}{2}\sum_{i=1}^{5}\int_{m_{cs}^{(i)}} \dot{\mathbf{r}}_{cs}^{(i)} \cdot \dot{\mathbf{r}}_{cs}^{(i)}\, \mathrm{d}m_{cs}^{(i)} + \frac{1}{2}\sum_{j}\left(m_j \dot{\mathbf{r}}_j \cdot \dot{\mathbf{r}}_j + \bar{\omega}_j^{\mathrm{T}} \bar{I}_j \bar{\omega}_j\right) + \frac{1}{2}\int_{m_{cr}} \dot{\mathbf{r}}_{cr} \cdot \dot{\mathbf{r}}_{cr}\, \mathrm{d}m_{cr}, \tag{4}$$

$$P.E. = \frac{1}{2}\sum_{i=1}^{5}\left[\int_{0}^{L_i} EI_i (W_{cs,\, z_i\, z_i})^2\, \mathrm{d}z_i + \int_{0}^{L_i} GJ_i (\phi_{,\, z_i})^2\, \mathrm{d}z_i\right] + \frac{1}{2}\int_{0}^{L_6} EI_6\, (W_{cr,\, x_6\, x_6})^2\, \mathrm{d}\, x_6$$

$$+\sum_{i=1}^{5}\int_{0}^{L_i}\rho\, A_i\, g\mathbf{I}\cdot\mathbf{r}_{cs}^{(i)}\,\mathrm{d}z_i+\int_{0}^{L_6}\rho\, A_6\, g\,\mathbf{I}\cdot\mathbf{r}_{cr}\,\mathrm{d}x_6+\sum_{j}(m_j g\,\mathbf{I}\cdot\mathbf{r}_j), \tag{5}$$

$$j=fl, cw1, cw2, gr, p$$

where the datum line is considered to coincide with the inertial Z-axis. The virtual work done by the non-conservative generalized forces is

$$\delta W_{NC}=-PA_p\mathbf{I}\cdot\delta\mathbf{r}_p+\int_{0}^{L_2}\left\{\mathbf{F}_{ax}^{(2)}\cdot\left[-\frac{1}{2}\,\delta\,(W_{cs,z_2}^{2})\,\mathbf{k}_2\right]\right\}\mathrm{d}z_2$$

$$+\int_{0}^{L_4}\left\{\mathbf{F}_{ax}^{(4)}\cdot\left[-\frac{1}{2}\,\delta\,(W_{cs,z_4}^{2})\,\mathbf{k}_4\right]\right\}\mathrm{d}z_4+\int_{0}^{L_6}\left\{\mathbf{F}_{ax}^{(6)}\cdot\left[-\frac{1}{2}\delta(W_{cr,x_6}^{2})\mathbf{i}_6\right]\right\}\mathrm{d}x_6+\delta W_f$$

$$-T_{load}\,\mathbf{K}\cdot[-\delta W_{cs,z_5}\,\mathbf{i}_5+W_{cs,z_5}\,\delta\theta\mathbf{j}_5+(\delta\theta+\delta\phi)\mathbf{k}_5]_{z_5=L_5}, \tag{6}$$

where the terms involving $\mathbf{F}_{ax}^{(i)}$ reflect the stiffening effect induced by the centripetal acceleration of the system. δW_f is the virtual work done by the friction forces and torques. It is defined as

$$\delta W_f=-(F_{rm}+F_{rv})\delta\,[T_0^7(x_{pr}^*\,y_{pr}^*\,z_{pr}^*\,|\,1)^{\mathrm{T}}]-F_{vt}\,\delta\,[T_0^7(x_7^*\,y_7^*\,z_7^*\,|\,1)^{\mathrm{T}}]$$

$$-F_{sk}\,\delta\,[T_0^7(x_{sk}^*\,y_{sk}^*\,z_{sk}^*\,|\,1)^{\mathrm{T}}]-(T_a+T_{lb})\left[\delta\theta+\frac{1}{2}\delta\phi\left(z_1=\frac{L_1}{2}\right)+\frac{1}{2}\delta\phi\left(z_5=\frac{L_5}{2}\right)\right], \tag{7}$$

where F_{rm} and F_{rv} represent the friction forces stemming from the boundary-mixed and the hydrodynamic lubrication regimes of the piston rings, respectively. F_{vt} is the friction force of the valve train. F_{sk} is the friction force due to the hydrodynamic lubrication regime of the piston skirt. T_a is the friction torque of the auxiliaries and unloaded bearings. T_{lb} is the friction torque of the loaded bearings. These terms are adopted from the work done by Rezeka and Henein [12]. Their expressions are slightly modified to suit the current formulation (see Table 1). It should be emphasized that any other engine friction model could have served the purpose of this study.

Note that three co-ordinates θ, β and γ have been used to represent the rigid body motion of the crank-slider mechanism. To deal with the superfluous co-ordinates, the following two constraint equations are imposed to prevent the piston from tilting or from moving away from the centerline of the cylinder in the **J**-direction:

$$\bar{\boldsymbol{\omega}}_p\cdot\mathbf{k}_7=0 \text{ and } \mathbf{r}_p^*(t)\cdot\mathbf{J}=\text{const.} \tag{8}$$

The equations of motion of the crank-slider mechanism are obtained by implementing the Lagrange principle. The equations can be written in the compact form

$$M(\mathbf{q})\,\ddot{\mathbf{q}}+\mathbf{F}(\mathbf{q},\dot{\mathbf{q}})=\mathbf{Q}^{NC}+\boldsymbol{\lambda}^{\mathrm{T}}\,s_1(\mathbf{q}), \tag{9}$$

TABLE 1
Frictional losses of the engine components

Ring Boundary-mixed	$F_{rm} = 0{\cdot}252\pi\ D\, n_{crg}\, w_{crg}\, (P + P_{e,crg})\ (1 - \lvert Sin(\theta)\rvert)$ $270^\circ \leqslant \theta \leqslant 450^\circ$
Ring Viscous lubrication	$F_{rv} = 23{\cdot}0\ [\mu \lvert V_p\rvert\, w_{crg}(P + P_{e,crg})]^{1/2}\ (1{\cdot}4\, n_{crg})\ D$
Skirt	$F_{sk} = \mu V_p\, D\, L_{skirt}/h$
Valve train	$F_{vt} = 0{\cdot}26\, n_{valve}\, SL/\sqrt{\dot{\theta}}$
Auxiliaries and unloaded bearings	$T_a = 9{\cdot}6\ \mu\theta$
Loaded bearings	$T_{lb} = 0{\cdot}5\ (\pi/4)\, D^2\, P \lvert Cos(\theta)\rvert (d_1/2)/\sqrt{\dot{\theta}}$

where $\mathbf{q}$ is defined to be $(\theta, \beta, \gamma, q_1, q_2, q_3, q_4)^{\mathrm{T}}$; s_1 is obtained by differentiating the constraint equations with respect to time and by writing the results as $s_1\, \ddot{\mathbf{q}} + \mathbf{s_2} = \mathbf{0}$. To handle the resulting set of differential-algebraic (D-A) equations, the Lagrange multiplier vector, $\boldsymbol{\lambda}$, is determined by implementing the scheme used in reference [15]. The equations of motion are then integrated numerically by using the Gear's stiff integrator. The reader is referred to references [14, 16] for further details on the dynamic model of the crank-slider mechanism.

It should be clarified that given the scope of the work described in this paper; one could have used the substitution method to eliminate the superfluous co-ordinates. However, the general form of differential-algebraic equations is used herein so that future work can build on the current formulation to consider the effects of hydrodynamic lubrication regimes inherent in the crank-slider mechanism.

3. DIGITAL SIMULATION RESULTS

The equations, presented in the previous section, are included in the upper block of Figure 1.The detailed model is used herein as a test bed to determine the overall frictional losses of the engine and to predict the combined rigid and flexible motions of the crank-slider mechanism. The (P–ω) formulation, inserted in the lower block of Figure 1, is obtained from the rigid body model of the crank-slider mechanism. It is used to estimate the instantaneous engine friction torque based on the measured angular velocity of the crankshaft, ω_a, the cylinder gas pressure, P, and the engine load torque, T_{load}.

By implementing the substitution method to eliminate the superfluous β and γ co-ordinates, the rigid body model of the crank-slider mechanism can be reduced to the following differential equation in θ:

$$J(\theta)\,\ddot{\theta} + \bar{F}(\theta, \dot{\theta}) = G(P, T_{load}) + T_{fe}, \tag{10}$$

where all the frictional losses of the crank-slider mechanism have been lumped into a single term, T_{fe}. The measurements of θ, P and T_{load} render all the terms in the above equation to become known quantities except for T_{fe}. Therefore, the (P–ω)

method uses equation (10) as an algebraic equation for estimating the instantaneous engine friction torque.

θ is usually measured by an optical encoder. The crankshaft angular velocity and acceleration are then obtained by differentiating the optical encoder signal with respect to time. Note that θ consists of the torsional vibration and the rigid body angular displacement of the crankshaft. Since the formulation of the (P–ω) method does not account for the structural deformations of the crank-slider mechanism, the torsional vibration component of the optical encoder signal is more likely to cause erroneous predictions of the frictional losses.

The objective of the current digital simulations is to manipulate the torsional vibration component of the measured angular velocity, ω_a, in an attempt to assess the individual or collective contributions of the crankshaft elastic modes on the estimation of the engine friction torque (see Figure 1).

A cylinder gas pressure trace, corresponding to engine firing conditions, and a constant load torque are considered in this study. These signals are used in the detailed model to determine the friction torque, T_{fa}, and to predict the rigid and flexible motions of the crank-slider mechanism. The T_{fa} plot, shown in Figure 3, is used here as a base for comparison.

To simulate the implementation of the (P–ω) method as presented in the literature, ω_a is considered to be $\omega_r + \sum_{i=1}^{3} \Phi_i(z_1 = 0)\,\dot{q}_i(t)$ (see Figure 1). A comparison of Figures 3 and 4 demonstrates that the estimated friction torque T_{fe} is close to T_{fa} during the first half of the first cycle. This is because the digital simulation starts from an undeformed configuration of the crank-slider mechanism. As a consequence, the crankshaft does not experience significant deformations until the first firing in the cylinder has occurred. Beyond that point, the T_{fe} plot greatly differs from that of T_{fa}. This is because the structural deformations start to play a larger role in the estimation of the friction torque. To support this argument, two

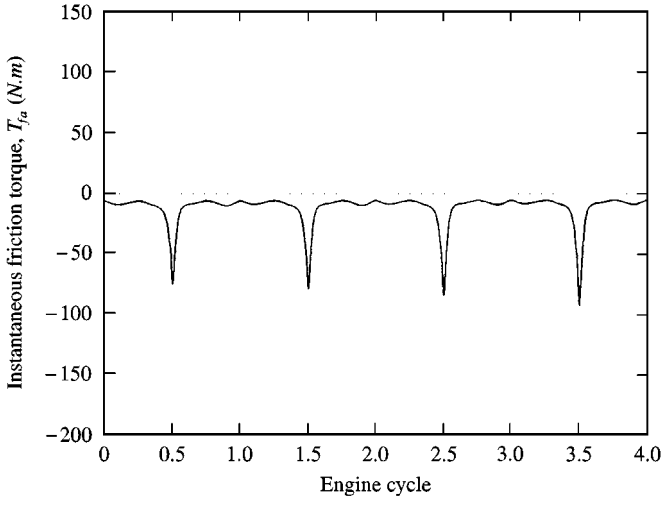

Figure 3. Instantaneous friction torque obtained from the detailed model of the crank-slider mechanism.

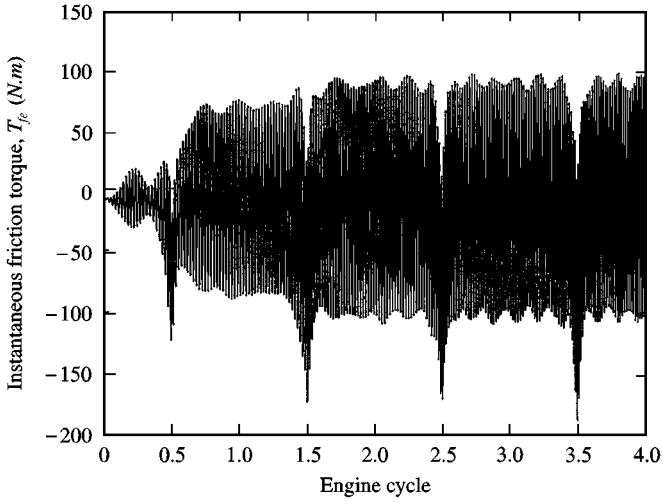

Figure 4. Instantaneous friction torque obtained from the (P–ω) method; $\omega_a = \omega_r + \sum_{i=1}^{3} \Phi_i$ $(z_1 = 0)\ \dot{q}_i\,(t)$.

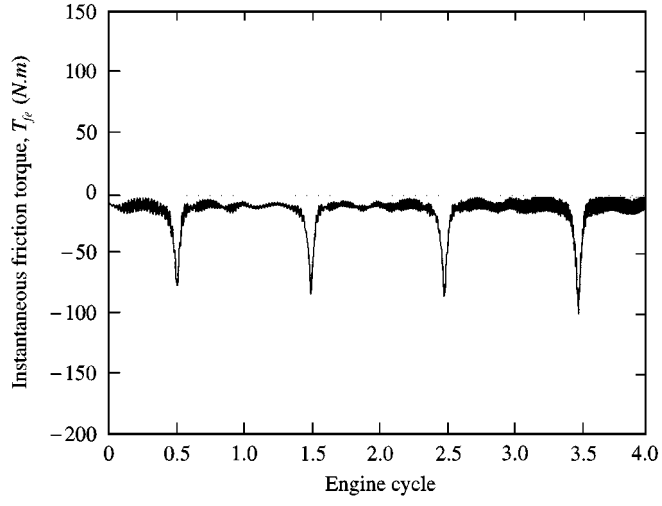

Figure 5. Instantaneous friction torque obtained from the (P–ω) method; $\omega_a = \dot{\omega}_r + \sum_{i=2}^{3} \Phi_i$ $(z_1 = 0)\ \dot{q}_i\,(t)$.

additional cases corresponding to $\omega_a = \omega_r + \sum_{i=2}^{3} \Phi_i (z_1 = 0)\, \dot{q}_i(t)$ and $\omega_a = \omega_r + \Phi_3\ (z_1 = 0)\, \dot{q}_3\,(t)$ have been considered. The T_{fe} results, illustrated in Figures 4–6, demonstrate that the first elastic mode of the crankshaft has the most significant contribution on the computation of the friction torque. Furthermore, Figure 6 shows that the effect of the third torsional mode on T_{fe} is insignificant. Thus, the third and higher order elastic modes of the crank-slider mechanism can be ignored from the formulation without compromising the accuracy of the estimated friction torque.

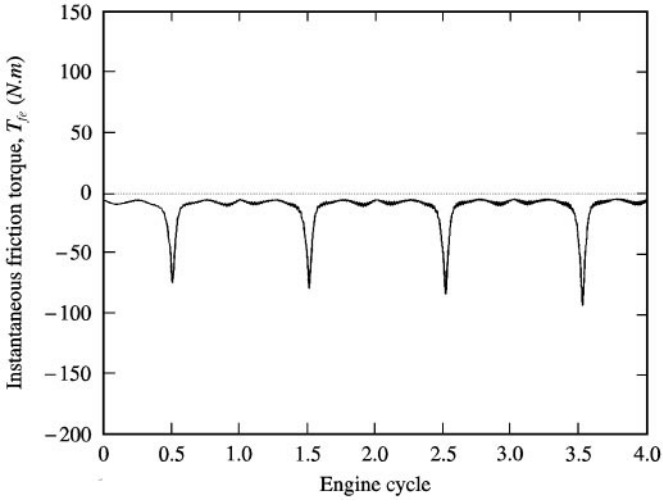

Figure 6. Instantaneous friction torque obtained from the (P–ω) method; $\omega_a = \omega_r + \Phi_3\ (z_1 = 0)\ \dot{q}_3\ (t)$.

Figures 3–5 serve to prove that the (P–ω) method tends to overestimate T_{fe} near the top-dead-center (TDC) position of the piston under firing conditions. The erroneous results stem from the fact that the (P–ω) method does not account for the structural deformations of the crank-slider mechanism. Near the TDC position of the piston, the crankshaft/connecting-rod/ piston mechanism will be subjected to high cylinder gas pressures that are induced by the combustion process. As a consequence, the system will undergo maximum deformations that can possibly occur during the engine cycle. The deformations, reflecting the strain energy stored in the crank-slider mechanism (see Figure 7), are introduced to the (P–ω) method through ω_a. Since the (P–ω) method does not have any provision in its formulation to account for the structural deformations, the strain energy stored in the crank-slider mechanism must appear as frictional losses. This causes T_{fe} to be overestimated near TDC position of the piston, which occurs halfway through the cycle.

Similar reasoning can be followed to explain the large oscillations and the positive numerical values of the friction torque. For the remainder of the engine cycle, the cylinder gas pressure is relatively small. Thus, the crank-slider mechanism will try to regain its undeformed configuration. During this process, the strain energy stored in the system will be released. Since the (P–ω) method does not handle structural deformations, the only source in the formulation that can account for the released energy would be T_{fe}. As a result, the estimated friction torque would take on positive values; thus, appearing as if it is injecting energy into the system.

Furthermore, Figure 8 exhibits the result of an interesting case whereby the engine friction torque is estimated by setting $\omega_a = \omega_r$. Under this condition, it would be reasonable to expect the T_{fe} plot of Figure 8 to exactly match that of T_{fa} in Figure 3. However, the results turned out to be slightly different. The reason for the differences in the plots stems from the fact that by setting $\omega_a = \omega_r$ one has only removed the direct effect of the crankshaft structural deformations, $\sum_{i=1}^{3} \Phi_i(z_1 = 0)\,\dot{q}_i(t)$, on ω_a.

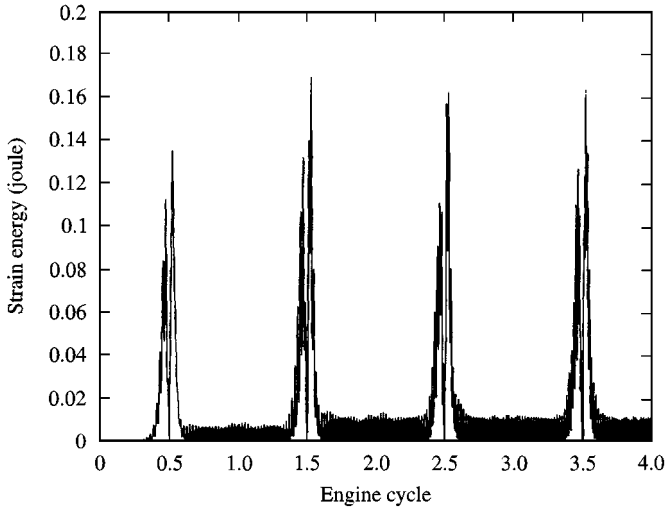

Figure 7. Strain energy stored in the crank-slider mechanism.

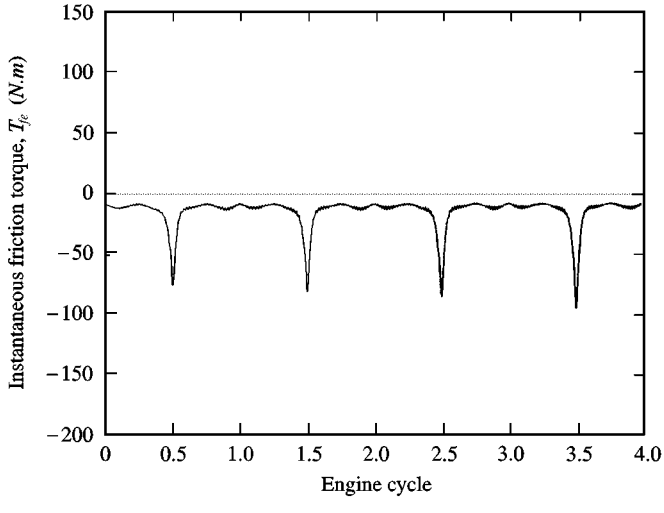

Figure 8. Instantaneous friction torque obtained from the (P–ω) method; $\omega_a = \omega_r$.

The measured angular velocity of the crankshaft is still indirectly influenced by the structural deformations of the crank-slider mechanism through ω_r. Even though the latter represents the rigid body angular velocity of the crankshaft, it is still affected by the structural deformations due to the strong coupling between the rigid and flexible motions of the crank-slider mechanism, which has a tendency to slightly alter the rigid body behavior of the system. This coupling effect, inherent in the physical system, is accounted for in the detailed model of the crank-slider mechanism by the presence of structural flexibility terms in the rigid body equations of motion of the system. Recalling that the (P–ω) method is based soley

on the rigid body motion of the crank-slider mechanism, then any direct and/or indirect effects of the structural flexibility on ω_a would have a tendency to induce errors in the results of the (P–ω) method. Thus, the differences between the plots in Figures 3 and 8 can be attributed to the indirect effect of structural deformations of the crank-slider mechanism on ω_a.

Similarly, the close match between Figures 6 and 8 reveals that the high-frequency oscillations in the T_{fe} plot of Figure 6 are mostly induced by the indirect effect of structural deformations on ω_a through ω_r rather than by the direct effect of the crankshaft third elastic mode.

4. SUMMARY AND CONCLUSIONS

The current study examines the effects of structural deformations of the crankshaft/connecting-rod/piston mechanism on the estimation of the engine friction torque. To isolate the effects of structural deformations, this work is performed in a fully controlled environment that is free from any measurement errors or noise interference. Therefore, a detailed model for the crank-slider mechanism of a single cylinder engine is used herein as a test bed to generate the instantaneous friction torque and to predict the rigid and flexible motions of the system in response to the cylinder gas pressure and a constant load torque. The model takes into consideration the torsional vibration and the out-of-plane transverse deformation of the crankshaft along with the out-of-plane transverse deformation of the connecting rod. In addition, the engine friction torque is determined based on the formulations provided by Rezeka and Henein [12] for the computation of the engine component frictional losses. It should be emphasized that any other engine friction model could have served the purpose of this study.

The (P–ω) method is well suited for the purpose of this work because its formulation is based on a rigid body model of the crank-slider mechanism. This methodology estimates the engine friction torque based on the measured signal of the cylinder gas pressure, P, the crankshaft angular velocity, ω_a, and the engine load torque, T_{load}. Both the (P–ω) method and the detailed model of the crank-slider mechanism are used herein according to the configuration shown in Figure 1. Note that the ω_a input of the (P–ω) method is defined in such a way that it simulates the signal usually obtained by differentiating the optical encoder signal with respect to time. The crankshaft torsional vibration component of ω_a is manipulated in this study to assess the individual as well as the collective contributions of the crankshaft elastic modes on the estimation of the instantaneous engine friction torque.

The digital simulation results have demonstrated that erroneous estimations of the instantaneous engine friction torque can be obtained if the structural deformations of the crankshaft/connecting-rod/piston mechanism are excluded from the formulation of the (P–ω) method. Near the firing TDC position of the piston, the strain energy of the crank-slider mechanism reaches its maximum value. During this period, the (P–ω) method has a tendency to overestimate the friction torque. Moreover, the absence of high gas pressure in the remainder of the engine cycle enables the crank-slider mechanism to regain its undeformed configuration.

The released strain energy is manifested by large oscillations and positive numerical values of T_{fe}; thus, appearing as if the engine friction torque is inducing energy into the system. Therefore, the effects of structural deformations on T_{fe} greatly differ from one phase of the engine cycle to another.

Furthermore, the strong coupling between the rigid and flexible motions of the crank-slider mechanism have slightly altered the rigid body behavior of the system. Consequently, ω_r becomes indirectly influenced by the structural deformations of the system which causes the (P–ω) method to yield erroneous results even in the case where ω_a is defined to be equal to ω_r. However, it should be emphasized that the error in T_{fe} induced by the indirect effect of structural deformations on ω_r is almost negligible in comparison to the one stemming from the inclusion of the first and second elastic modes of the crankshaft in ω_a.

ACKNOWLEDGMENT

The authors would like to acknowledge the financial support of the Automotive Research Center (consortium of five universities directed by the University of Michigan) by the National Automotive Center, located within the U.S. Army Tank-Automotive Research, Development, and Engineering Center (TARDEC), Warren, Michigan.

REFERENCES

1. R. C. Rosenberg 1976 *SAE Paper* 821576. General Friction Considerations for Engine Design.
2. J. A. McGeehan 1973 *SAE Paper* 780673. A literature review of the effects of piston and ring friction and lubricating oil viscosity on fuel economy.
3. K. Shin, Y. Tateishi and S. Furuhama 1985 *Institute of Mechanical Enginering* **3**, 87–94. Measurement and characteristics of instantaneous piston ring frictional force.
4. M. Takiguchi, K. Machida and S. Furuhama 1988 *ASME Journal of Tribology* **110**, 112–118. Piston friction force of a small high speed gasoline engine.
5. H. M. Uras and D. J. Patterson 1983 *SAE Paper* 830416. Measurement of piston and ring assembly friction instantaneous IMEP method.
6. N. A. Henein, 1992 *Technical Report*, *Mechanical Engineering Department*, *Wayne State University*. Instantaneous engine frictional torque, its components and piston assembly friction.
7. B. W. Millington and E. R. Hartles 1968 *SAE Paper* 680590. Friction losses in diesel engines.
8. N. A. Henein, A. Fragoulis and A. Nichols 1988 *Journal of the Society of Tribologists and Lubrication engineers* **44**, 313–318. Time-dependent frictional torque in reciprocating internal combustion engines.
9. Y. G. Ku 1987 *Ph.D. Dissertation*, *University of Michigan*. A study of piston and ring friction in an internal combustion engine.
10. S. S. Lin 1993 *Ph.D. Dissertation*, *University of Michigan*. Piston/ring assembly friction measurement and modeling.
11. D. Taraza, N. A. Henein and W. Bryzik 1996 *SAE Paper* 962006. Experimental determination of the instantaneous frictional torque in multi-cylinder engines.
12. S. F. Rezeka and N. A. Henein 1984 *SAE Paper* 840179. A new approach to evaluate instantaneous friction and its components in internal combustion engines.
13. L. Meirovitch 1986 *Elements of Vibration Analysis*. New York: McGraw-Hill.

14. H. NEHME, N. G. CHALHOUB and N. A. HENEIN 1998 *ASME Journal of Engineering for Gas Turbines and Power* **120–3**, 678–686. Development of a dynamic model for predicting the rigid and flexible motions of the crank slider mechanism.
15. C. GLOCKER and F. PFEIFFER 1992 *Nonlinear Dynamics* **3**, 245–259. Dynamical systems with unilateral contacts.
16. N. G. CHALHOUB, H. NEHME, N. A. HENEIN and W. BRYZIK 1998 in Proceedings of the 1998 *ASME International Mechanical Engineering Congress and Exposition, Dynamic Systems and Control Division* **64**, 657–664. Role of the crank-slider structural deformations in the prediction of the instantaneous engine friction torque.

APPENDIX: NOMENCLATURE

A_i, m_i	cross-sectional area and mass of the ith beam element respectively
D, d_1	diameters of the cylinder bore and the journal bearing respectively
EI_i	flexural rigidity of the ith beam element
$\mathbf{F}(\mathbf{q}, \dot{\mathbf{q}})$	vector containing inertial, stiffness and gravitational acceleration terms
$\bar{F}(\theta, \dot{\theta})$	represents inertial and gravitational acceleration terms in the rigid body model of the crank-slider mechanism
$G(P, T_{load})$	non-conservative generalized forces due to the cylinder gas pressure and the load torque
GJ_i	torsional stiffness of the ith beam element
g, ρ	gravitational acceleration and density respectively
h, P	oil film thickness and cylinder gas pressure respectively
$(\mathbf{I}, \mathbf{J}, \mathbf{K})$	unit vectors along the axes of the inertial co-ordinate system
$\bar{I}_j$	inertia tensor of the jth rigid body
$J(\theta)$	inertia term in the rigid body model of the crank-slider mechanism
L_i, L_{skirt}	length of the ith beam element and the piston skirt respectively
$M(\mathbf{q})$	inertia tensor in the detailed model of the crank-slider mechanism
n_{crg}, n_{valve}	numbers of compression rings and valves, respectively
$P_{e,crg}$	pressure due to the elastic deformation of the compression ring
$\mathbf{Q}^{NC}$	non-conservative generalized force vector
$\mathbf{q}_f$	vector consisting of the structural flexibility generalized co-ordinates $[q_1 \ q_2 \ q_3 \ q_4]^T$
SL	valve spring load
T_{fa}, T_{fe}	actual and estimated engine friction torques respectively
T_{load}, V_p	engine load torque and piston velocity respectively
W_{cr}, W_{cs}	out-of-plane transverse deformations of the connecting-rod and the crankshaft respectively
w_{crg}	average width of the compression ring
θ, β, γ	angular displacements of the crankshaft, the connecting-rod and the piston respectively
μ	dynamic viscosity of the lubricant
ϕ, Φ_i	torsional vibration and ith eigenfunction of the crankshaft respectively
ω_r	rigid body angular velocity of the crankshaft
ω_a	measured angular velocity of the crankshaft
$\bar{\boldsymbol{\omega}}_j$	rotation vector of the jth rigid body
$()_{cr}$, $()_{cs}$	"*cr*" and "*cs*" subscripts refer to variables associated with the connecting-rod and the crankshaft respectively
$()_{cwi}$	a "*cwi*" subscript indicates a variable associated with the ith counterweight
$()_{fl}$, $()_{gr}$	"*fl*" and "*gr*" subscripts denote variables that are associated with the flywheel and the crank gear respectively
$()_p$, $()_{pr}$	"*p*" *and* "*pr*" subscripts refer to variables that are associated with the piston mass center and the piston rings respectively

$()_{sk}$	a "*sk*" subscript refers to a variable that is associated with the piston skirt
$()_{,z_i}$	a "$,z_i$" subscript indicates partial differentiation with respect to z_i
$()^*$	a "*" superscript refers to a variable that is associated with the mass center